Title
PHASE SHIFTS FOR p-4He ELASTIC SCATTERING BETWEEN 20 AND 40 MeV

Authors
Plattner, G.R.
Bacher, A.D.
Conzett, H.E.

Publication Date
1971-12-01

Submitted to Physical Review

LBL-269
Preprint

PHASE SHIFTS FOR p-^{4}He ELASTIC SCATTERING BETWEEN 20 AND 40 MeV

G. R. Plattner, A. D. Bacher and H. E. Conzett

December 1971

AEC Contract No. W-7405-eng-48

DISCLAIMER

Phase shifts for p-^{4}He elastic scattering between 20 and 40 MeV[+]

G.R.Plattner

Physics Department, University of Basel, 4056 Basel, Switzerland

A.D.Bacher[++] and H.E.Conzett

Lawrence Berkeley Laboratory, University of California, California 94720

ABSTRACT

A phase shift analysis of recent p-^{4}He cross-section and polarization data has been performed between 20 and 40 MeV proton laboratory energy. A set of single energy results is presented, which shows little scatter as a function of energy. The match between our results and existing phase shift sets below 20 and above 40 MeV is excellent. The most striking feature of the phase shifts above the inelastic threshold at 23.02 MeV is the dominance of absorption in the even partial waves. There is weak evidence in the energy dependence of the phase shifts for levels of ^{5}Li other than the well known $3/2^+$ second excited state. Tentative assignments of spin and parity of such levels are discussed. An R-matrix parametrization of the $^2D_{3/2}$ phase shift has been performed over the p-^{4}He resonance corresponding to the second excited state of ^{5}Li, and improved level parameters are presented for this state.

I. INTRODUCTION

This paper is the second part of a report on p-^{4}He elastic scattering between 20 and 40 MeV. The first paper [1] describes the experimental results, which provide an accurate set of polarization and cross-section data. In this second paper we present the results of a phase-shift analysis.

Phase-shift analyses of p-^{4}He elastic scattering are numereous and quite reliable for the energy region below 20 MeV (refs. 2-4 and references therein). They reflect the abundance and high precision of the available data.

Above the inelastic threshold near 23 MeV, both the quantity and quality of experimental data [5-9] on p-^{4}He scattering have until recently been inferior to the information available in the low-energy region. This has primarily been due to the lack of intense polarized beams. Analyses are further hampered: (1) by the increasing importance of higher partial waves, (2) by the need to consider complex rather than real phase shifts above the inelastic threshold, and (3) by the lack of detailed knowledge of inelastic processes leading to three or more particles in the final state.

Though considerable effort has gone into the derivation of p-^{4}He phase shifts above 20 MeV [6,8,9-15], these difficulties have lead to inconsistent and contradictory results. In particular it has not been possible to deduce reliable information about the highly excited states of ^{5}Li from the analyses presented

up to this time. Only the $3/2^+$ second excited state near 16.7 MeV excitation has been investigated with some precision [8,9].

The results presented in this paper show that our p-^{4}He polarization and cross-section data above 20 MeV proton laboratory energy allow a consistent phase-shift analysis to be performed, which permits at least a qualitative discussion of the properties of possible states in ^{5}Li above 18 MeV excitation and also provides an improved parametrization of the $3/2^+$ second excited state.

II. PHASE-SHIFT ANALYSIS

A. Formalism

The expressions linking the observable quantities $\sigma(\Theta)$ (differential cross-section), σ_T (total inelastic cross-section) and $p(\Theta)$ (polarization) in spin 1/2-spin zero elastic scattering to the nuclear phase shifts are well known and have been given repeatedly in the literature (for σ and p see refs. 14 and 16, for σ_T see ref. 8).

Apart from using relativistically correct expressions for all kinematical variables, we have also taken into account first order relativistic corrections to the Coulomb-amplitude according to the method proposed by Foote et.al. [16] in an analysis of π^+-p elastic scattering [17]. These corrections are by no means negligible in our energy range, since in some instances they amount to effects of 1-2% in the observables.

B. Search Program

In order to find single-energy phase-shift solutions, a gradient-search routine was used. As a measure of the quality of fit, the usual quantity χ^2 per datum point was used [3], which included contributions due to the differential cross-section (χ^2_σ), the polarization (χ^2_p), and the total inelastic cross-section if available.

The only uncommon feature of our search program consisted in an option to let both the polarization and the differential cross-section be renormalized after each step along the gradient of χ^2. The renormalization factors f_p and f_σ were calculated in such a way, that after renormalization the quantity M given by

$$M = \chi^2_p + \left(\frac{f_p - 1}{\Delta f_p}\right)^2 + \chi^2_\sigma + \left(\frac{f_\sigma - 1}{\Delta f_\sigma}\right)^2$$

was a minimum. In this expression χ^2_p (χ^2_σ) denotes the quality-of-fit criterion per datum point of the experimental polarization (cross-section) after renormalization, and the quantity Δf_p (Δf_σ) is the normalization uncertainty of the experimental polarization (cross-section) angular distribution as given in ref. 1.

C. Input Data

Experimental information on both differential cross-section and polarization was taken exclusively from our own recent measurements [1]. The main reason for this preference lies in the superior quality of our polarization data over older measurements obtained without

the benefit of intense polarized proton beams. As mentioned in ref. 1, there are no serious discrepancies between our data and that of other authors.

Our cross-section data are favored at this point simply because they have been taken simultaneously with the polarization data and thus no energy differences exist between the two. In addition, the previously existing cross-section data are quite sparse and in most cases not drastically better than our own. The absolute normalization, which is the principal uncertainty of our data, does not seem to be much more reliable for the older measurements [9,18-21].

The available information on the total inelastic cross-section σ_T of ^{4}He for protons is very sparse and partly inconsistent. Between the inelastic threshold (d+^{3}He) at 23.02 MeV and the first three-body threshold (2p+t) near 24.9 MeV, σ_T can be obtained from the total cross-section of the ^{3}He(d,p)^{4}He reaction using detailed balance. Unfortunately, the measurements of this cross-section [22-27] below the 2p+t threshold differ by as much as 30%. Though arguments can be put forward which tend to favour the data of ref. 22, no strong constraint on the imaginary parts of the p-^{4}He phase shifts can be obtained below 25 MeV. We have used the data of ref. 22 as an input in the phase-shift searches. The weight of their contributions to χ^2 was chosen to equal that of two of our own data points.

Above the lowest three-body threshold, the experimental information on σ_T becomes even more sparse. A lower limit can again be set via detailed balance from the $^3He(d,p)^4He$ data [28]. At 28 MeV, above the 2p+t and p+n+^{3}He thresholds, a value of 14.7 ± 1.6 mb has been reported [29] for the total cross-section leading to these two final states. The only other measurements [30,31] near our energy range have been performed well above all inelastic thresholds at 53 and 55 MeV. Values for σ_T of 107.7 ± 4.4 mb and 105 ± 15 mb respectively have been found at these energies.

Through these few experimental points a smooth curve for $\sigma_T(E)$ was drawn by hand. The values thus obtained were then used with 10% error bars as an input for the phase shift searches. The weight of their contributions to χ^2 was chosen to equal that of two of our own data points up to 30 MeV, and that of eight above that energy.

D. Procedure

Single energy phase-shift analyses were carried out starting at 20 MeV. As a starting set of phase shifts, values extrapolated from the energy-dependent set of ref. 3 were used. After a solution was found at one energy, the corresponding best fit phase shifts were taken as starting values for a search on the data at the next higher energy.

This procedure yielded satisfactory fits with seven parameters (real s, p, d, and f-wave phase shifts) at the first four energies up to the inelastic threshold near 23 MeV. Above this threshold, 14 parameters (complex s,p,d, and f-wave phase shifts) were used. In this manner, a smoothly energy-dependent set of phase shifts was obtained over the $3/2^+$ resonance corresponding to the second excited state of ^{5}Li. Above 24.5 MeV, the quality of the fits deteriorated gradually, until the continuous solution was lost at 30 MeV.

Since g-wave are expected to become important above 30 MeV, the search was extended to include 18 parameters (complex s,p,d,f, and g-wave phase shifts), starting at 26 MeV. The quality of the fits was immediately improved and no problems were encountered in proceeding to 40 MeV. For the purpose of indentification, the set of single-energy phase-shift solutions found in this manner will be called set I.

At this stage, smooth curves were drawn by hand through the set I phase shifts as a function of energy, and a second string of single-energy searches (now including g-waves at all energies) was undertaken from 20 to 40 MeV with the smoothed set I phase shifts as starting points. This resulted in the set II single-energy solutions, which not only were more smoothly dependent on energy, but also gave a better overall fit to the data.

Set II was modified once more before arriving at the final results. An R-matrix calculation was performed to parametrize the complex $^2D_{3/2}$ phase shift between 20 and 32 MeV in an attempt to extract level parameters for the second excited state of ^{5}Li. The details of this investigation are given in section III. In the present context we need only say, that a third string of single-energy searches was performed. Between 20 and 32 MeV, we started from set II, but with the $^2D_{3/2}$ phase shift fixed at the values predicted by the R-matrix calculation. At energies above 32 MeV the $^2D_{3/2}$ parameters were initially set to values extrapolated from the R-matrix predictions at the lower energies. No problem was encountered in finding slightly modified solutions (set III) at all energies with little increase in χ^2.

Set III represents the final result of our phase-shift analysis of p-^{4}He elastic scattering. It is presented in section IV and will be discussed in section V.

III. R-MATRIX PARAMETRIZATION OF THE $^2D_{3/2}$ PHASE-SHIFT

A. Motivation

Two R-matrix calculations concerned with the influence of the $3/2^+$ second excited state in ^{5}Li on p-^{4}He elastic scattering have been published previously [8,9]. In order to understand why we have reexamined this effect, it is instructive to anticipate the final result of our R-matrix calculation as presented in fig. 1.

In this figure, the real phase $\delta = \mathrm{Re}(^2D_{3/2})$ and the absorption parameter $\eta = \exp(-2\,\mathrm{Im}(^2D_{3/2}))$ are shown. The solid lines correspond approximately to the empirical phase shift parameters (i.e. to the set II values), whereas the dotted lines give a fair representation of the shape of a well-behaved, isolated resonance [32]. The unusual feature of our empirical $^2D_{3/2}$ phase shift lies in the "cut-off" of resonance effects in the real part on the high energy side of the resonance. A similar, corresponding feature can be seen in our polarization data [1] at the same energy, so that there can be little doubt as to the existence of this effect.

In both previous investigations [8,9] of this resonance the authors have oversimplified their R-matrix analysis by completely neglecting resonance-background interference. As we will show, it is just this contribution which produces the peculiar resonance shape, so that a more sophisticated R-matrix analysis of the $^2D_{3/2}$ phase shift is called for.

B. Method

Our analysis is based strictly on the formalism as presented by Lane and Thomas [35] and we will use their notation in this section. We will not attempt to list all the pertinent formulae, but will only try to explain simplifying assumptions. For the details of the theory the reader is referred to ref. 35.

In order to calculate the $^2D_{3/2}$ phase shift from the assumed properties of the $3/2^+$ second excited state of ^{5}Li and of the non-resonant background, we have constructed the symmetric 3x3 (3-channel) R-matrix $R^{3/2}$ with elements

$$R_{cc'} = \frac{\gamma_c \gamma_{c'}}{E_\lambda - E} + R^o_{cc'}(E) \qquad (1)$$

The entrance and exit channel indices c and c' refer to the three channels

(1) $p + {}^4He$ ($\ell = 2$, $s = 1/2$)
(2) $d + {}^3He$ ($\ell = 0$, $s = 3/2$)
(3) $d + {}^3He$ ($\ell = 2$, $s = 1/2$ and $3/2$)

The quantity E_λ is the c.m. characteristic energy [36] of the $3/2^+$ level in the $p+{}^4He$ channel. The quantity γ_c is the reduced width amplitude of this level in channel c, and E designates the c.m. kinetic energy in the $p+{}^4He$ channel. The non-resonant background is represented by the parameters $R^o_{cc'}(E)$, which have been chosen to depend linearly on energy:

$$R^o_{cc'}(E) = R^o_{cc'} + (dR^o/dE)_{cc'}(E - 18.353) \qquad (2)$$

Thus $R^o_{cc'}(E)$ equals $R^o_{cc'}$ at 18.353 MeV, the c.m. energy of the first inelastic threshold.

The matrix $R^{3/2}$ was then inserted into eqs. VII, 1.6a and 1.5 of ref. 35 and the collision matrix element $U_{11}{}^{3/2}$, corresponding to elastic scattering in the $^2D_{3/2}$ $p+^4He$ channel, was calculated [37]. Finally, the real phase δ and the absorption parameter η, corresponding to the complex $^2D_{3/2}$ phase shift, were obtained from

$$\eta \exp (2i\delta + 2i\omega) = U_{11}{}^{3/2} \qquad (3)$$

where $\omega = \sigma_2 - \sigma_0$, the difference between the Coulomb phase shifts for $\ell = 2$ and $\ell = 0$.

The interaction radii a_c were chosen as

$$a_1 = \quad 3.0 \text{ fm } (p+^4He \text{ channel}), \quad \text{and}$$

$$a_2 = a_3 = 5.0 \text{ fm } (d+^3He \text{ channels}).$$

In all three channels the boundary condition B_c on the internal eigenfunctions (ref. 35, IV, 2) was chosen such that the shift factor S^o was equal to zero at the characteristic energy E_λ of the $3/2^+$ level:

$$B_c = S_c(E_\lambda) \quad , \quad S_c^o(E_\lambda) = S_c(E_\lambda) - B_c = 0. \qquad (4)$$

This choice is discussed in detail in section XII of ref. 35 and implies that the observed resonance energy E_R of the $3/2^+$ level coincides with the characteristic energy E_λ.

The following simplifications were made as compared to the most general many-channel case:

(1) Only three channels have been taken into account. We have thus made no distinction between the two possible channel spins of the d-wave d+^{3}He channel and have completely neglected breakup channels, which all have thresholds in or near the energy range of interest. It is hoped that the influence of the neglected channels can implicity be absorbed into the three channels considered [38].

(2) The background terms have been chosen to depend linearly on energy. In order to reduce the number of parameters, the following additional assumptions were made:

$$R^o_{33}(E) = R^o_{22}(E)\ ,\ R^o_{23}(E) = 0,\ R^o_{13}(E) = R^o_{12}(E) \qquad (5)$$

so that only $R^o_{11}(E)$, $R^o_{22}(E)$, and $R^o_{12}(E)$ remain independent. A set of six parameters was thus taken to describe the non-resonant background. The relations (5) amount to: (1) ascribing the same intrinsic amplitude to non-resonant d-^{3}He elastic scattering in channels with $\ell = 0$ and $\ell = 2$ and neglecting transitions between them, and (2) ascribing the same intrinsic non-resonant amplitude to the transitions p+^{4}He $\longrightarrow$ d+^{3}He ($\ell = 0$) and p+^{4}He $\longrightarrow$ d+^{3}He ($\ell = 2$). Such simplifying assumptions are necessary to keep the number of

parameters in manageable proportions, but they are admittedly quite arbitrary and at best reasonable.

C. Results of R-Matrix Calculation

We first tried to obtain a fit to an empirical background phase shift as determined by drawing a smooth curve, neglecting resonance effects, through the empirical values for the $^2D_{3/2}$ parameters δ and η. After a satisfactory background phase shift had been generated, a set of $3/2^+$ level parameters was included in the calculation and a search was performed in an attempt to reproduce the complete $^2D_{3/2}$ phase shift. A good fit could be obtained both on and off resonance with little need for change in the background parameters determined previously. Since resonance and background interfere quite strongly, such a behaviour seems to imply that the background has reasonable properties. This in turn constitutes a strong a posteriori justification of the simplifying assumptions made.

On the average, the resulting energy-dependent $^2D_{3/2}$ phase shift agreed to better than $\pm 0.5^\circ$ in δ and ± 0.02 in η with the empirical values between 14 and 32 MeV (ref. 3 below 20 MeV, set II above 20 MeV). The maximum discrepancies, occuring right on resonance at 23.3 MeV, were 2.6° in δ and 0.06 in η. After folding in the experimental energy resolution of our data [40], this discrepancy was reduced to an amount compatible with a shift in energy of the 23.29 MeV empirical phase shift by $\pm$ 20 keV, i.e. by less than the stated uncertainty of the experiment [1].

Since they are part of solution set III, the folded R-matrix results for the $^2D_{3/2}$ phase shift are tabulated in table II along with the empirical values for the other partial waves. The R-matrix parameters used in the calculation are given in table I. In fig. 1, both δ and η are plotted as a function of energy. The solid lines are the result of our calculation for both level plus background, while the dashed lines show the background only. The double arrow marks the resonance energy. The dotted lines demonstrate the importance of resonance-background interference. They show the result that one would predict from our parameters as listed in table I, if this interference were completely neglected, i.e. if one were to use the method [41] of refs. 8 and 9. In contrast to our calculation, it is probably not possible with this method to reproduce the strong "cut-off" effect that our data require.

Fig. 2 shows a comparison between the experimental data for the total cross-section σ_T of the $^3He(d,p)^4He$ reaction [22] and the values calculated from our R-matrix parameters. Again the dashed line indicates the calculated background contribution. The agreement is excellent, considering that there may be small contributions from other J-values than $3/2^+$, which are missing from our calculation. A slight apparent energy shift between experiment and calculation is well within the combined uncertainties in energy of our data [1] and those of ref. 22.

The properties of the $3/2^+$ second excited state of ^{5}Li as determined by our calculation are in qualitative agreement with those deduced from a study [8] of the ^{3}He(d,p)^{4}He total cross-section and those obtained in a simplified analysis [9] of p-^{4}He scattering data. The reduced width of this state for decay into one of the d+^{3}He channels is approximately equal to the Wigner limit, whereas the proton width is only about 1.5% of this limit. Consequently this state is of almost pure d+^{3}He character, similar to the more conventional nucleon-core single particle states, and has been called a cluster state. According to our results, it seems to have approximately equal contributions from d+^{3}He structures with $\ell = 0$ and $\ell = 2$. It must be stated, though, that our analysis is not very sensitive to the assumed width for decay into the $\ell = 2$ channel.

IV. RESULT OF THE PHASE-SHIFT ANALYSIS

The numerical values of solution set III are listed in table II. Also given there are the corresponding calculated values for the total inelastic cross-section σ_T, the quantity χ^2 per datum point for the differential cross-section (χ^2_σ), the polarization (χ^2_p), and for both observables together ($\chi^2_{\sigma+p}$). In addition, the normalization factors f_σ and f_p as determined by the search routine (see section II,B) are shown. It should be remembered, that these normalization factors indicate the amount by which the experimental data have been corrected to give the χ^2-values listed in table II.

In figs. 3 and 4, the p-^{4}He phase shifts are shown as a function of energy from 0-50 MeV. The solid lines below 18 MeV represent the energy-dependent set of phase shifts of ref. 3. The solid line between 18 and 32 MeV for the $^2D_{3/2}$ phase shift is the result of our R-matrix calculation. Otherwise, our phase shifts are shown as open and full circles indicating δ and η, respectively. The triangles at 48 MeV represent the results of ref. 14. To guide the eye, dashed lines have been drawn through the single-energy values.

In figs. 5 and 6, fits to the experimental data are shown at four energies. The data points represent our unnormalized experimental data [1]. The calculated fits, renormalized by $1/f_\sigma$ and $1/f_p$ are plotted as solid lines.

In fig. 7, fits to the polarization across the 23.4 MeV resonance are shown. The full circles are our data [1]; the solid lines represent the values calculated from the set of single-energy phase shifts listed in table II.

In fig. 8, the experimental polarization excitation function at $\theta_{cm} = 102.2^\circ$ is compared with the values calculated from our phase shifts. The broad anomaly centered around 30 MeV is well reproduced by the dashed line, which has been drawn through the calculated values. In this figure, the open circles are from ref. 9, the full circles and squares represent our own data, and the closed and open triangles are from refs. 6 and 7, respectively.

V. DISCUSSION

In the following discussion we will assume that the phase shifts as presented in section IV are a good approximation to the hypothetical "true" p-^{4}He phase shifts. We have not made any efforts to find other solutions, but as far as the real parts δ of our phase shifts are concerned, the continuity from 0-50 MeV is a convincing argument for this assumption. As is evident from the scatter of the values for the absorption parameters η (see figs. 3 and 4), they are less well determined by the data. While our solution reproduces the total inelastic cross-section of ^{4}He for protons as well as it is known (see section II, C), more accurate measurements of this quantity would be of great help. However, the very good match between the trend of our parameters and the independently determined RHEL phase shifts [14] at 48 MeV gives us additional confidence in our solution.

One feature of our phase shifts, which is not entirely satisfactory, should be mentioned at this point. Below 26 MeV the absolute cross-sections predicted from our final solution are on the average 7-8% higher than those determined experimentally [9,18-21]. We have looked for phase-shift solutions which would require a less sizeable renormalization of the cross-section, but were unsuccessful. This is indeed an unfortunate situation, and since there are some inconsistencies in the data used for normalization, we feel that only a careful absolute cross-section measurement spanning the energy range from approximately 15-30 MeV can clear up the discrepancies.

Discussing the implications of our phase-shift results for the level structure of ^{5}Li, we should note that the weak anomaly discovered in our polarization measurements around 30 MeV (see fig. 8) is <u>not</u> connected with a particular feature of any one phase-shift parameter, but rather seems to be caused by the rapid onset of absorption above the inelastic threshold.

This result is in striking disagreement with a recent analysis [15] of p-^{4}He elastic scattering data[19] between 25 and 29 MeV, where rapid variations with energy of both the $^2S_{1/2}$ and the $^2D_{5/2}$ phase shifts have been found and are interpreted as conclusive evidence for the existence of two excited states around 20 MeV in ^{5}Li with $J^{\pi} = 1/2^+$ and $5/2^+$.

We have tried to reproduce our own data [1] in that energy region with phase shifts similar to those presented in ref. 15, but could find no acceptable, quantitative fits. On the other hand, our smoothly energy dependent phase shifts seem to satisfactorily reproduce the data of ref.19 (shown there only in figures). We therefore feel that no excited levels of ^{5}Li above the second excited state at 16.7 MeV have yet been unambiguously identified via a study of the p+^{4}He channel.

In a broader, less definite way we do agree, however, that the influence of highly excited states in ^{5}Li is probably seen in the p+^{4}He channel. The most striking feature of our phase shifts is certainly the dominance of absorption in the even partial waves. Absorption of protons from the p+^{4}He channel is not distributed between the partial waves in the way one would expect

if simple potential scattering were dominant. Around 30 MeV (corresponding to 22 MeV excitation in ^{5}Li), absorption in the $J^{\pi} = 1/2^+$, $3/2^+$, $5/2^+$, and $7/2^+$ scattering states amounts to 85% of the total inelastic cross-section. This behaviour can be understood qualitatively, if it is assumed that at these energies there exist in ^{5}Li very broad, overlapping levels of positive parity, which decay almost exclusively via the d+^{3}He and/or multiparticle-breakup channels.

Recent calculations with a refined cluster model have indeed led Heiss and Hackenbroich [42] to predict the existence in ^{5}Li of a quartet of T = 1/2 states with $J^{\pi} = 1/2^+$, $3/2^+$, $5/2^+$, and $7/2^+$. These states are calculated to be of almost pure d-wave d+^{3}He character and are situated several MeV above the d+^{3}He threshold. Their nature is very similar to that of the $3/2^+$ second excited state of ^{5}Li, which is also reproduced in these calculations [42,43].

Further experimental support for this theoretical prediction is presented by Tanifuji and Yazaki [44], who report that the effective potential between deuterons and ^{3}He, needed to describe elastic scattering, is very much stronger in the even than in the odd parity states at an energy corresponding to 22 MeV excitation in ^{5}Li.

Additional evidence for positive parity states in this energy range is found by Seiler [45] in an investigation of the ^{3}He(d,p)^{4}He reaction. He reports that a state with $J^{\pi} = 5/2^+$ near 20 MeV excitation and one with $J^{\pi} = 7/2^+$ near 22.5 MeV dominate this process.

Our own investigation of p-^{4}He elastic scattering is not in contradiction with the possible existence of a $7/2^+$ level. In this scattering state we see an anomaly in the energy dependence of our phase shift ($^2G_{7/2}$). However, to deduce the existence of a $7/2^+$ level solely from these very weak fluctuations would not be justified.

Turning now to a discussion of the odd partial waves, we find that our p-wave phase shifts, which correspond to $J^\pi = 1/2^-$ and $3/2^-$, show some fluctuations again in the absorptive parts, while the f-wave phases with $J^\pi = 5/2^-$ and $7/2^-$ are completely without structure.

Empirical evidence for $J^\pi = 1/2^-$ and $3/2^-$ levels has been obtained from studies of the ^{3}He(d,p)^{4}He reaction [45,46], of d-^{3}He elastic scattering [47], of its mirror process d-T elastic scattering [48], and of the ^{3}He(d,2p)T and T(d,pn)^{3}T reactions [49]. The cluster-model calculation by Heiss and Hackenbroich [42] also generated such states and explains them as nucleon +^{4}He* (0^+ first excited state) cluster structures, which would decay mainly into multiparticle-breakup channels. The coupling to p+^{4}He channels should be very weak according to this model.

If all this tentative evidence for highly excited states in ^{5}Li is taken at face value, then the following qualitative picture of ^{5}Li (and mutatis mutandis of ^{5}He) emerges from the existing experimental information:

Ground and first excited states are pure single particle states consisting of a p-wave proton in the potential well of a closed s-shell α-particle (which gives rise to the repulsive "hardsphere" interaction evident in the p-^{4}He s-wave phase shift).

Proton single particle states with orbital angular momenta $\ell > 1$ will be situated somewhere above 30 MeV excitation, but their influence can be seen below that energy in the gradual rise of the real parts of the d, f, and g-wave p-^{4}He phase shifts. Due to their high excitation they are extremely broad and strongly overlapping. The sign of the spin-orbit splitting of all these states is in accordance with the shell model ordering.

Above the first inelastic threshold, near 16.5 MeV, a series of broad d+^{3}He cluster states appears. The first of these is the $3/2^+$ second excited state, which has been unambiguously identified. Its relatively small width is only a consequence of its position close to threshold. Its inherent character is that of a cluster state with a reduced with close to the Wigner limit. Above 18 MeV excitation, a quartet of d-wave d+^{3}He cluster states with $J^\pi = 1/2^+$, $3/2^+$, $5/2^+$, and $7/2^+$, and a doublet of p+^{4}He* cluster states with $J^\pi = 1/2^-$ and $3/2^-$ are predicted to exist[42]. Experimental evidence for all of these states is still inconclusive, however, despite claims to the contrary [15,49].

In our opinion, a phase-shift analysis of the existing experimental information on d-^{3}He elastic scattering and a detailed investigation of multiparticle-breakup reactions such as ^{3}He(d,2p)T are the two most promising approaches to further study the level structure of the five nucleon system at high excitation.

6. ACKNOWLEDGEMENTS

We wish to express our thanks to Prof.E.Baumgartner, Prof.W.Haeberli, Dr.F.Seiler and Dr.Th.Stammbach for many valuable discussions. We are grateful to Dr.P.Heiss, Prof.M.Tanifuji, and Dr.F.Seiler for sending us results of their work prior to publication.

References

+ Work supported in part by the Swiss National Science Foundation and by the U.S. Atomic Energy Commission.

++ Present address: Physics Department, Indiana University, Bloomington, Indiana 47401.

1 A.D.Bacher, G.R.Plattner, H.E.Conzett, D.J.Clark, H.Grunder, and W.F.Tivol, submitted to Physical Review.

2 G.R.Satchler, L.W.Owen, G.L.Morgan, and R.L.Walter Nucl.Phys. A112, 1 (1968).

3 P.Schwandt, T.B.Clegg, and W.Haeberli, Nucl.Phys. A163, 432 (1971).

4 R.A.Arndt, L.D.Roper, and R.L.Shotwell, Phys.Rev. C3, 2100 (1971).

5 C.F.Hwang, D.H.Nordby, S.Suwa, and J.H.Williams, Phys.Rev.Lett. 9, 104 (1962).

6 E.T.Boschitz, M.Chabre, H.E.Conzett, H.E.Shield, and R.J.Slobodrian, in Proceedings of the Second International Symposium on Polarization Phenomena of Nucleons, Karlsruhe, Germany, 1965, edited by P.Huber and H.Schopper (Experienta Suppl. 12, 1966), p. 328; and Phys.Lett. 15, 325 (1965).

7 M.K.Craddock, R.C.Hanna, L.P.Robertson, and B.W.Davies, Phys.Lett. 5, 335 (1963).

8 W.G.Weitkamp and W.Haeberli, Nucl.Phys. 83, 46 (1966).

9 P.Darriulat, D.Garreta, A.Tarrats, and J.Testoni, Nucl.Phys. A108, 316 (1968).

10 J.L.Gammel and R.M.Thaler, Phys.Rev. 109, 2041 (1958).

11 C.C.Giamati, V.K.Madsen, and R.M.Thaler, Phys.Rev.Lett. 11, 163 (1963).

12 S.Suwa and K.Yokosawa, Phys.Lett. 5, 351 (1963

13 C.C.Giamati and R.M.Thaler, Nucl.Phys. 59, 159 (1964).

14 B.W.Davies, M.K.Craddock, R.C.Hanna, Z.J.Moroz, and L.P.Robertson, Nucl.Phys. A97, 241 (1967).

15 K.Ramavataram, D.J.Plummer, T.K.Hodges, and D.G.Montague, Nucl.Phys. A174, 204 (1971).

16 J.H.Foote, O.Chamberlain, E.H.Rogers, and H.M.Steiner, Phys.Rev. 122, 959 (1961).

17 In order to adapt the formulae of ref. 16 to p-^{4}He elastic scattering, we have simply replaced quantities referring to π^+ by the corresponding quantities for ^{4}He in their equations (5) and (6) and taken into account the double charge of the ^{4}He nucleus. In all other respects we have used the expressions exactly as given in ref. 16.

18 P.W.Allison and R.Smythe, Nucl.Phys. A121, 97 (1968).

19 D.J.Plummer, K.Ramavataram, T.K.Hodges, D.G.Montague, K.Zucker, and N.K.Ganguly, Nucl.Phys. A174, 193 (1971).

20 S.M.Bunch, H. H. Forster, and C.C.Kim, Nucl.Phys. 53, 241 (1964).

21 M.K.Brussel and J.H.Williams, Phys.Rev. 106, 286 (1957).

22 J.L.Yarnell, R.H.Lovberg, and W.R.Stratton, Phys.Rev. 90, 292 (1953).

23 T.W.Bonner, J.P.Conner, and A.B.Lillie, Phys.Rev. 88, 473 (1952).

24 A.P.Kliucharev, B.N.Esel'son, and A.K.Val'ter, Doklady (Soviet Physics) 1, 475 (1956).

25 W.E.Kunz, Phys.Rev. 97, 456 (1955).

26 D.L.Booth, R.S.Hill, F.V.Price, and D.Roaf, Proc.Phys.Soc. A70, 863 (1957).

27 G.Freier and H.Holmgren, Phys.Rev. 93, 825 (1954).

28 L.Stewart, J.E.Brolley, Jr., and L.Rosen, Phys.Rev. 119, 1649 (1960).

29 A.F.Wickersham, Jr., Phys.Rev. 107, 1050 (1957).

30 D.J.Cairns, T.C.Griffith, G.J.Lush, A.J.Metheringham, and R.H.Thomas, Nucl.Phys. 60, 369 (1964).

31 S.Hayakawa, K.Matsuda, S.Nagata, and Y.Sumi, J.Phys.Soc.Jap. 19, 2004 (1964).

32 For a level with an elastic width $\Gamma_{el} < \frac{1}{2}\Gamma_{total}$, the resonating phase shift has this shape and does not pass through $\pi/2$ (see refs. 8, 33 and 34).

33 A.C.L.Barnard, J.S.Duval, Jr., and J.B.Swint, Phys.Lett. 20, 412 (1966).

34 B.Hoop, Jr., and H.H.Barschall, Nucl.Phys. 83, 65 (1966).

35 A.M.Lane and R.G.Thomas, Revs.Mod.Phys. 30, 825 (1958).

36 Relativistic expressions were used to convert kinematical variables from the laboratory to the center-of-mass system.

37 In this context we wish to thank Dr.G.Baur and Mr.F.Roesel for letting us use their Coulomb and Whittaker function computer codes.

38 The photo channel $\gamma + {}^5Li$ has also been omitted. This is of no consequence, however, since this channel has essentially no overlap with particle channels, as shown e.g. by the negligibly small cross-section [39] of the process ${}^3He(d,\gamma){}^5Li$.

39 L.Kraus, M.Suffert, and D.Magnac-Valette, Nucl.Phys. A109, 593 (1968).

40 Since for small variations of δ and η the observables can be expressed approximately as linear functions of the parameter increments, we took the experimental energy resolution [1] of $\pm$ 40 keV into account by simply folding a triangular weight distribution of 80 keV FWHM with the calculated values for δ and η.

41 These authors modify the single level, no background R-matrix expression of ref. 35 by replacing the hard-sphere phase shift with a phenomenological, complex, non-resonant background parameter. This results in complete neglect of the resonance-background interference.

42 P.Heiss and H.Hackenbroich, Nucl.Phys. A162, 530 (1971).

43 P.Heiss and H.Hackenbroich, Phys.Lett. 30B, 373 (1969).

44 M.Tanifuji and K.Yazaki, to be published, and private communication.

45 F.Seiler, private communication.

46 W.Grüebler, V.König, A.Ruh, P.A.Schmelzbach and, R.E.White, Proceedings of the Third International Symposium on Polarization Phenomena in Nuclear Reactions, Madison 1970, edited by H.H.Barschall and W.Haeberli (University of Wisconsin Press, Madison, 1970) p. 543.

47 V.König, W.Grüebler, R.E.White, P.A.Schmelzbach, and P.Marmier, Proc.Third Pol.Symp., ref.cit., p. 526.

48 K.Kilian, H.Treiber, R.Strausz, and D.Fick, Phys.Lett. 34B, 283 (1971).

49 D.Fick, H.Treiber, K.K.Kern, and H.Schröder. paper submitted to the Conference on the Nuclear Three-Body Problem, Budapest, Hungary, July 1971; and D.Fick, private communication.

Figure Captions

fig. 1 The $^2D_{3/2}$ phase shift in the vicinity of the $3/2^+$ second excited state of ^5Li. The solid lines represent the result of an R-matrix calculation. The dashed lines show the background contribution. The dotted lines are obtained, if resonance-background interference is neglected. The double arrow marks the resonance energy.

fig. 2 Comparison of the calculated values for σ_{tot} of the $^3He(d,p)^4He$ reaction with the experimental data of ref. 22. The solid line represents the result of an R-matrix calculation. The dashed line shows the background contribution.

fig. 3 s- and p-wave phase shifts for p-^{4}He elastic scattering. The solid lines below 18 MeV represent the energy-dependent set of phase shifts of ref. 3. Open and full circles are our own results for the real parts δ and the absorption parameter η, respectively. The triangles at 48 MeV indicate the results of ref. 14.

fig. 4 d, f, and g-wave phase shifts for p-^{4}He elastic scattering. See caption to fig. 3 for explanation of symbols.

fig. 5 Comparison at 24 and 26 MeV between our experimental data [1] and the corresponding curves calculated from the phase shifts of table II.

fig. 6 Comparison at 28 and 30 MeV between our experimental data [1] and the corresponding curves calculated from the phase shifts of table II.

fig. 7 Comparison of measured and calculated polarization excitation functions across the 23.4 resonance corresponding to the $3/2^+$ second excited state of ^{5}Li. The solid lines have been drawn through the values calculated from our single-energy phase-shifts as listed in table II.

fig. 8 Comparison between measured and calculated polarization at $\Theta_{cm} = 102.2^o$ across the broad anomaly near 30 MeV proton energy. Open circles are from ref. 3, full circles and squares are our own data [1]. The full and open triangles represent data from refs. 6 and 7, respectively. The dashed line has been drawn through the values calculated from our single-energy phase shift as listed in table II.

TABLE I. R-matrix parameters [a] used in the analysis of the $3/2^+$ second excited state of ^{5}Li.

E_R	$E_x(^5Li)$	$(\gamma_1)^2$	$(\gamma_2)^2$	$(\gamma_3)^2$	$(\theta_1)^2$	$(\theta_2)^2$	$(\theta_3)^2$	$(\theta_2)^2/(\theta_1)^2$	$\sum(\theta_i)^2$
23.39 MeV[b]	16.68 MeV	122 keV	1580 keV[c]	1580 keV	0.014[d]	0.765[d]	0.765[d]	55	1.55

R^o_{11}	$(dR^o/dE)_{11}$	R^o_{12}	$(dR^o/dE)_{12}$	R^o_{22}	$(dR^o/dE)_{22}$	a_1	a_2	a_3
0.468	0.008 MeV^{-1}	0.132	0.006 MeV^{-1}	0.187	-0.023 MeV^{-1}	3 fm	5 fm	5 fm

[a] The indices 1, 2, and 3 refer to the channels $p+^4He$ ($\ell = 0$), $d+^3He$($\ell = 0$), and $d+^3He$ ($\ell = 2$), respectively.

[b] Proton lab. energy in the $p+^4He$ channel.

[c] The sign of this reduced width amplitude is negative.

[d] In units of the Wigner limit $3\hbar^2/2Ma^2$.

Table II: Single-energy phase shift and related quanitities for p-^{4}He elastic scattering between 20 and 40 MeV

	19.94	21.90	23.46	22.71	22.96	23.16 MeV		23.29 MeV		23.48 MeV	
	δ	δ	δ	δ	δ	δ	η	δ	η	δ	η
$^2S_{1/2}$	94.01°	91.61°	91.13°	90.45°	90.12°	89.48°	1.000	89.73°	1.000	89.95°	1.000
$^2P_{3/2}$	94.24°	92.04°	90.92°	90.52°	90.15°	89.87°	1.000	89.65°	0.992	89.56°	0.994
$^2P_{1/2}$	56.00°	54.29°	53.28°	53.05°	52.95°	53.01°	1.000	53.35°	1.000	53.10°	1.000
$^2D_{5/2}$	6.30°	7.54°	7.67°	7.90°	7.85°	8.41°	1.000	8.66°	1.000	8.47°	1.000
$^2D_{3/2}$	4.67°	6.77°	8.17°	9.46°	11.10°	15.36°	0.980	19.40°	0.715	7.44°	0.636
$^2F_{7/2}$	1.96°	2.61°	2.97°	2.77°	2.89°	2.80°	1.000	3.47°	0.995	3.53°	1.000
$^2F_{5/2}$	1.73°	2.04°	2.26°	2.16°	2.17°	1.94°	1.000	3.24°	0.999	2.85°	0.995
$^2G_{9/2}$	-0.2°	0.24°	0.31°	0.22°	0.03°	0.11°	1.000	0.58°	1.000	0.53°	1.000
$^2G_{7/2}$	-0.1°	0.29°	0.33°	0.35°	0.15°	0.07°	1.000	0.69°	1.000	0.79°	1.000
σ_T						3.5 mb		46.2 mb		53.9 mb	
f_σ	1.070	1.043	1.101	1.093	1.129	1.083		1.068		1.064	
f_P	0.999	0.998	0.998	1.000	1.000	1.000		0.999		0.996	
χ^2_σ	0.39	0.66	0.97	0.69	1.25	0.33[a]		0.41		1.31	
χ^2_P	0.43	0.33	1.21	0.84	0.57	0.62		0.94		0.57	
$\chi^2_{\sigma P}$	0.41	0.49	1.09	0.77	0.91	0.73		0.68		0.94	

[a] value obtained without including forward most angle $\Theta_{cm} = 21.9°$

Table II: (cont'd)

	23.56 MeV		23.70 MeV		23.85 MeV		23.98 MeV		24.51 MeV		25.82 MeV	
	δ	η	δ	η	δ	η	δ	η	δ	η	δ	η
$^2S_{1/2}$	88.99°	1.000	89.07°	0.999	88.70°	0.998	88.14°	0.992	87.86°	1.000	87.23°	0.991
$^2P_{3/2}$	89.41°	0.997	89.54°	1.000	89.15°	0.997	89.60°	1.000	88.63°	0.994	88.99°	0.993
$^2P_{1/2}$	52.55°	1.000	52.65°	1.000	52.67°	1.000	52.10°	1.000	51.54°	1.000	51.06°	0.999
$^2D_{5/2}$	8.54°	0.995	9.00°	1.000	9.30°	0.995	9.81°	0.999	9.90°	0.993	10.93°	0.995
$^2D_{3/2}$	5.88°	0.695	5.44°	0.755	5.60°	0.786	5.77°	0.800	6.18°	0.814	6.45°	0.794
$^2F_{7/2}$	3.11°	1.000	3.26°	1.000	3.49°	0.997	3.64°	0.999	3.97°	1.000	4.11°	0.983
$^2F_{5/2}$	2.47°	1.000	2.65°	1.000	2.99°	1.000	3.08°	1.000	3.41°	1.000	3.60°	0.999
$^2G_{9/2}$	0.00°	1.000	0.17°	0.998	0.39°	1.000	0.41°	1.000	0.74°	1.000	0.73°	0.997
$^2G_{7/2}$	0.29°	1.000	0.22°	1.000	0.51°	1.000	0.62°	1.000	0.93°	1.000	1.34°	0.989
σ_T	46.4 mb		37.8 mb		35.6 mb		31.7 mb		30.7 mb		46.0 mb	
f_σ	1.077		1.095		1.076		1.037		1.091		1.043	
f_P	0.996		1.000		0.997		0.997		0.993		0.999	
χ_σ	1.15		0.64		0.58		0.29		0.36		0.37	
χ'_P	0.15		0.50		0.65		0.80		0.92		0.53	
$\chi_{\sigma+P}$	0.65		0.57		0.61		0.54		0.64		0.45	

Table II: (cont'd)

	28.13 MeV		30.43 MeV		32.17 MeV		34.30 MeV		36.93 MeV		39.80 MeV	
	δ	η	δ	η	δ	η	δ	η	δ	η	δ	η
$^2S_{1/2}$	85.01°	0.995	83.06°	0.940	81.64°	0.935	80.24°	0.909	77.54°	0.872	75.76°	0.842
$^2P_{3/2}$	84.08°	0.971	80.95°	0.957	78.60°	0.963	76.54°	0.961	73.56°	0.953	70.64°	0.940
$^2P_{1/2}$	48.35°	0.960	46.99°	0.954	45.53°	0.953	44.13°	0.961	41.70°	0.982	39.69°	1.000
$^2U_{5/2}$	12.71°	0.950	14.03°	0.882	14.85°	0.869	15.91°	0.826	17.61°	0.800	19.50°	0.771
$^2D_{3/2}$	6.73°	0.744	7.43°	0.705	8.35°	0.687	9.40°	0.675	10.57°	0.664	12.00°	0.655
$^2F_{7/2}$	5.05°	0.997	6.67°	0.990	7.93°	0.971	9.64°	0.966	11.47°	0.948	13.11°	0.917
$^2F_{5/2}$	4.50°	0.995	5.86°	0.995	6.79°	0.992	7.90°	0.983	8.78°	0.970	9.17°	0.953
$^2G_{9/2}$	1.01°	1.000	1.40°	1.000	2.09°	1.000	1.82°	0.998	2.03°	1.000	2.25°	0.992
$^2G_{7/2}$	1.25°	0.962	1.04°	0.975	1.13°	0.983	0.97°	0.973	0.83°	0.967	0.71°	0.962
σ_T	85.7 mb		78.7 mb		80.9 mb		89.9 mb		96.2 mb		106.1 mb	
f_T	1.068		0.990		0.997		0.996		1.001		1.000	
f_P	1.002		1.000		0.999		1.000		1.000		1.000	
χ'_T	0.52		0.91		0.62		1.03		1.03		0.67	
χ'_P	0.45		0.55		0.90		0.55		1.05		1.05	
$\chi_{S_{1/2}}$	0.50		0.73		0.76		0.79		1.04		0.87	

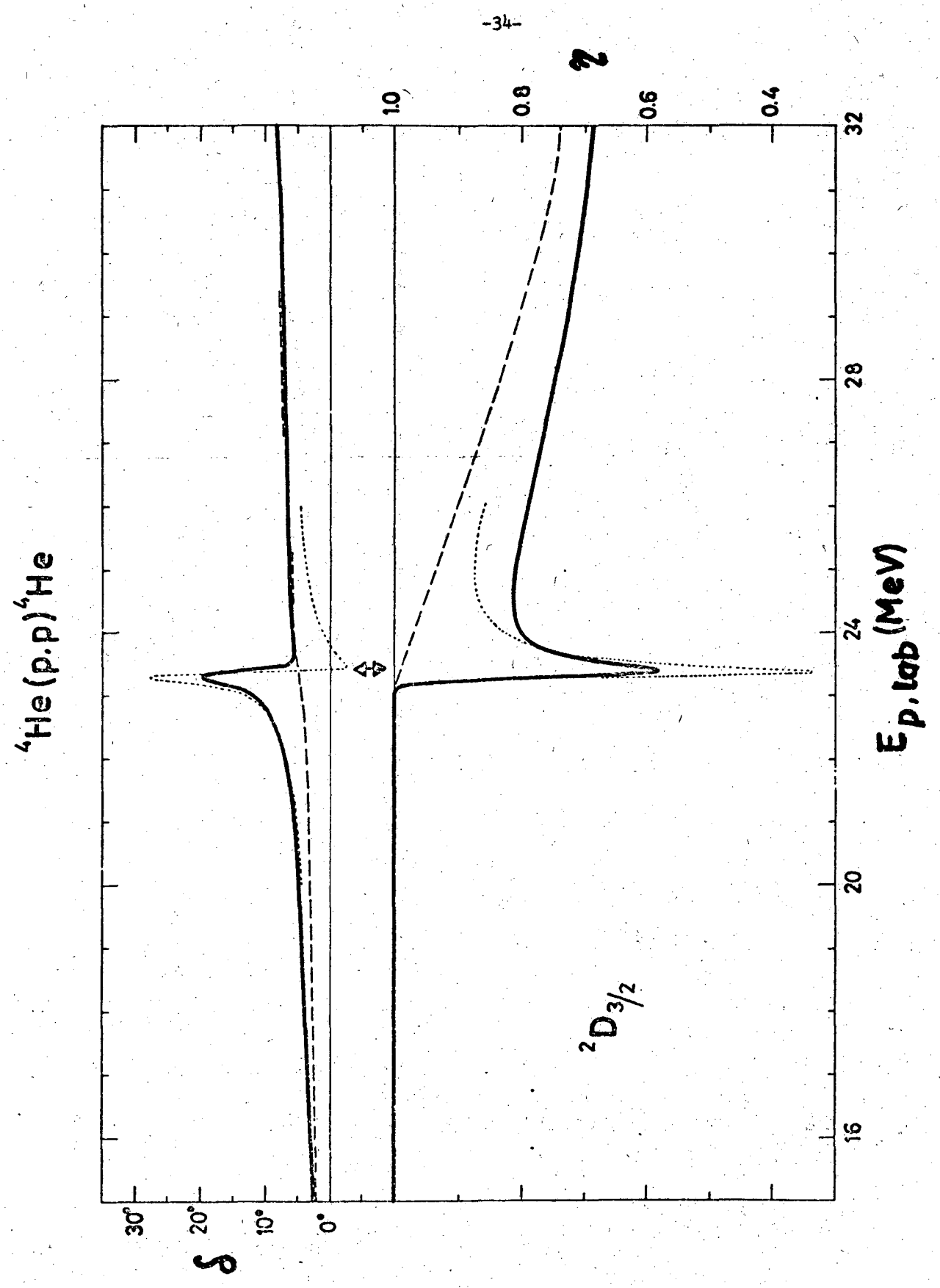

Fig. 1

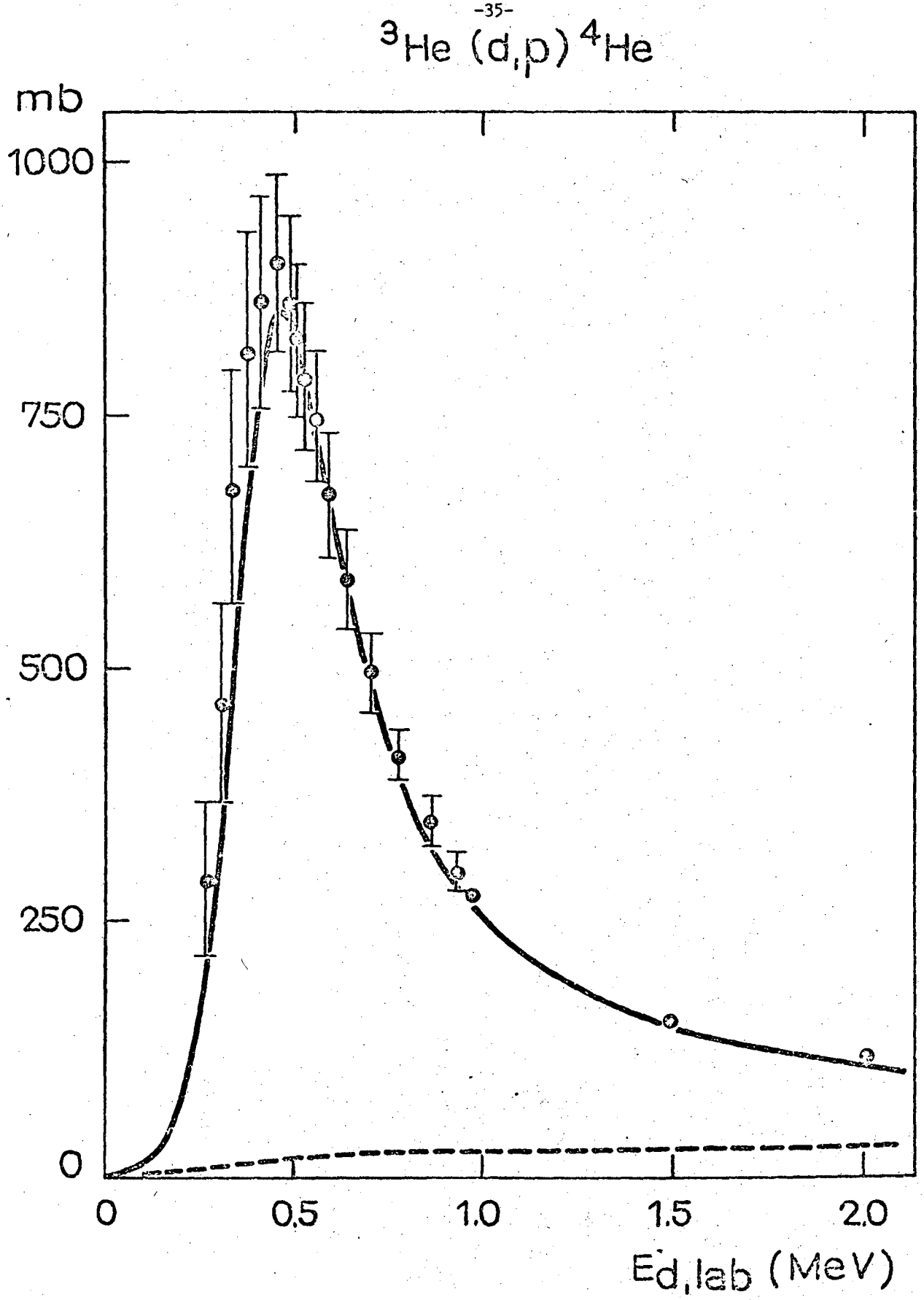

Fig. 2

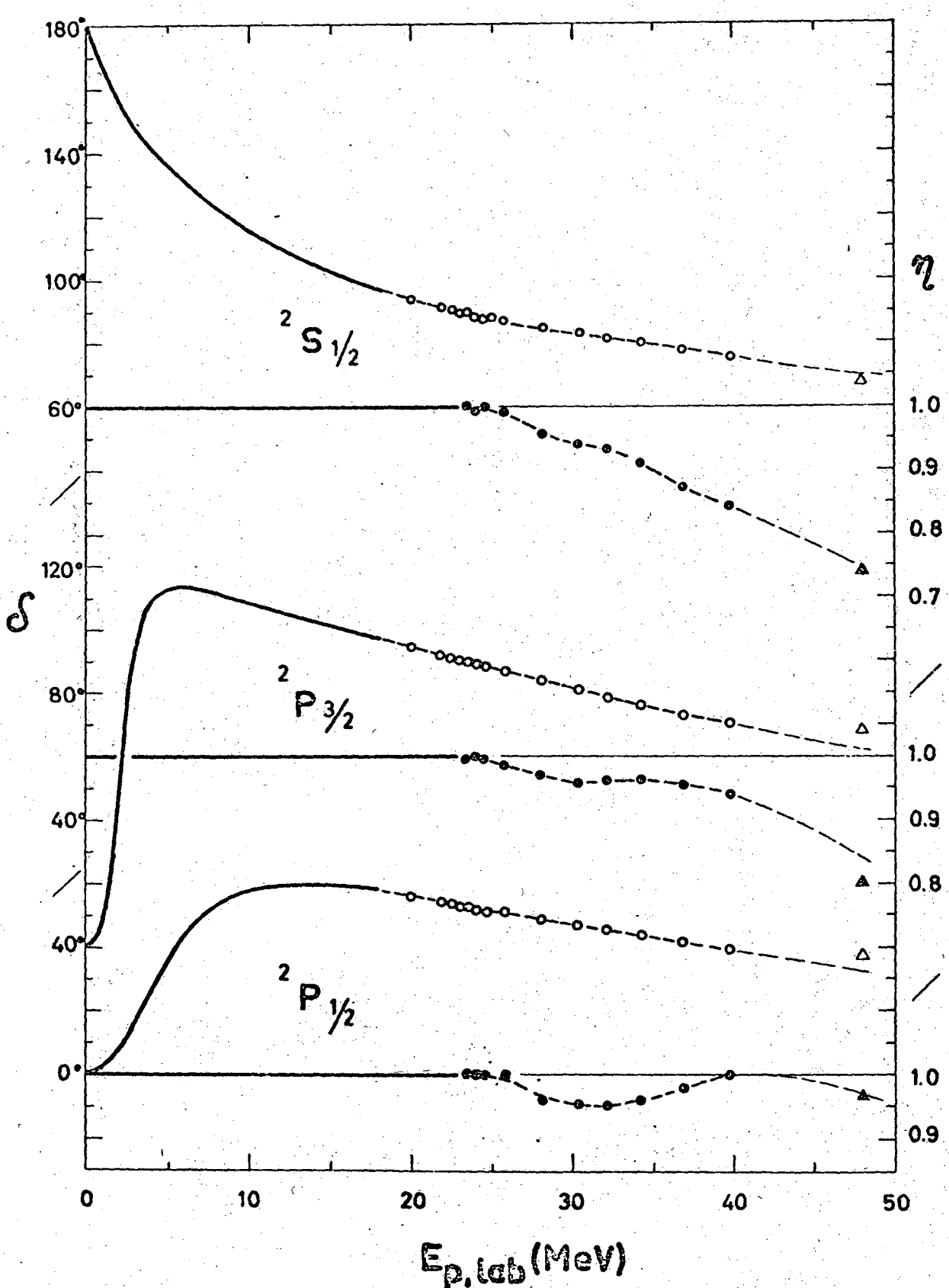
^{4}He (p,p) ^{4}He
180°
140°
100°
60°
120°
80°
40°
40°
0°
δ
η
^{2}S 1/2
^{2}P 3/2
^{2}P 1/2
1.0
0.9
0.8
0.7
1.0
0.9
0.8
1.0
0.9
0
10
20
30
40
50
$E_{p,lab}$ (MeV)

Fig. 3

$^4He(p,p)^4He$

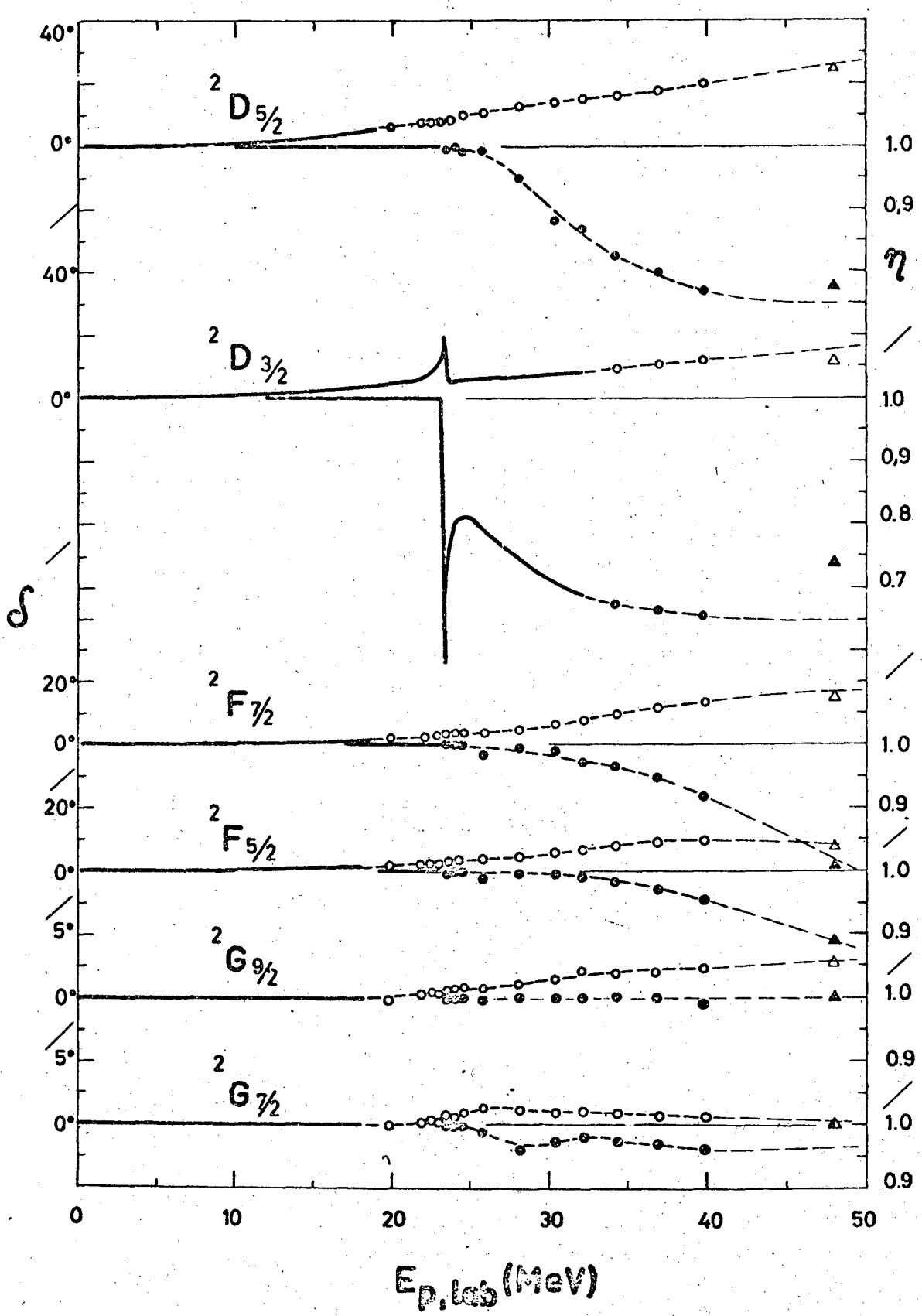

Fig. 4

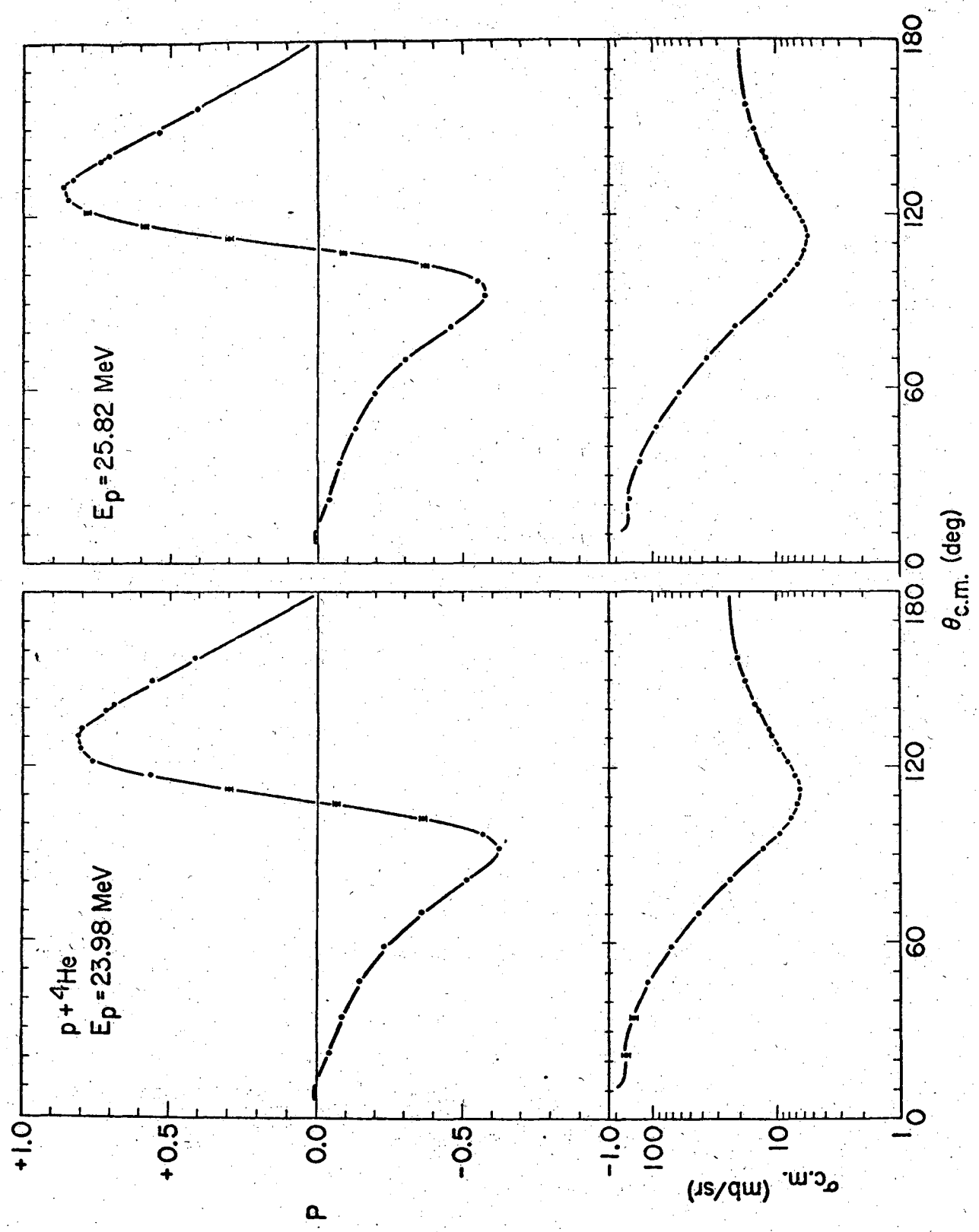
p + 4He
Ep = 23.98 MeV
Ep = 25.82 MeV
P
σc.m. (mb/sr)
θc.m. (deg)
+1.0
+0.5
0.0
-0.5
-1.0
100
10
1
0
60
120
180

Fig. 5

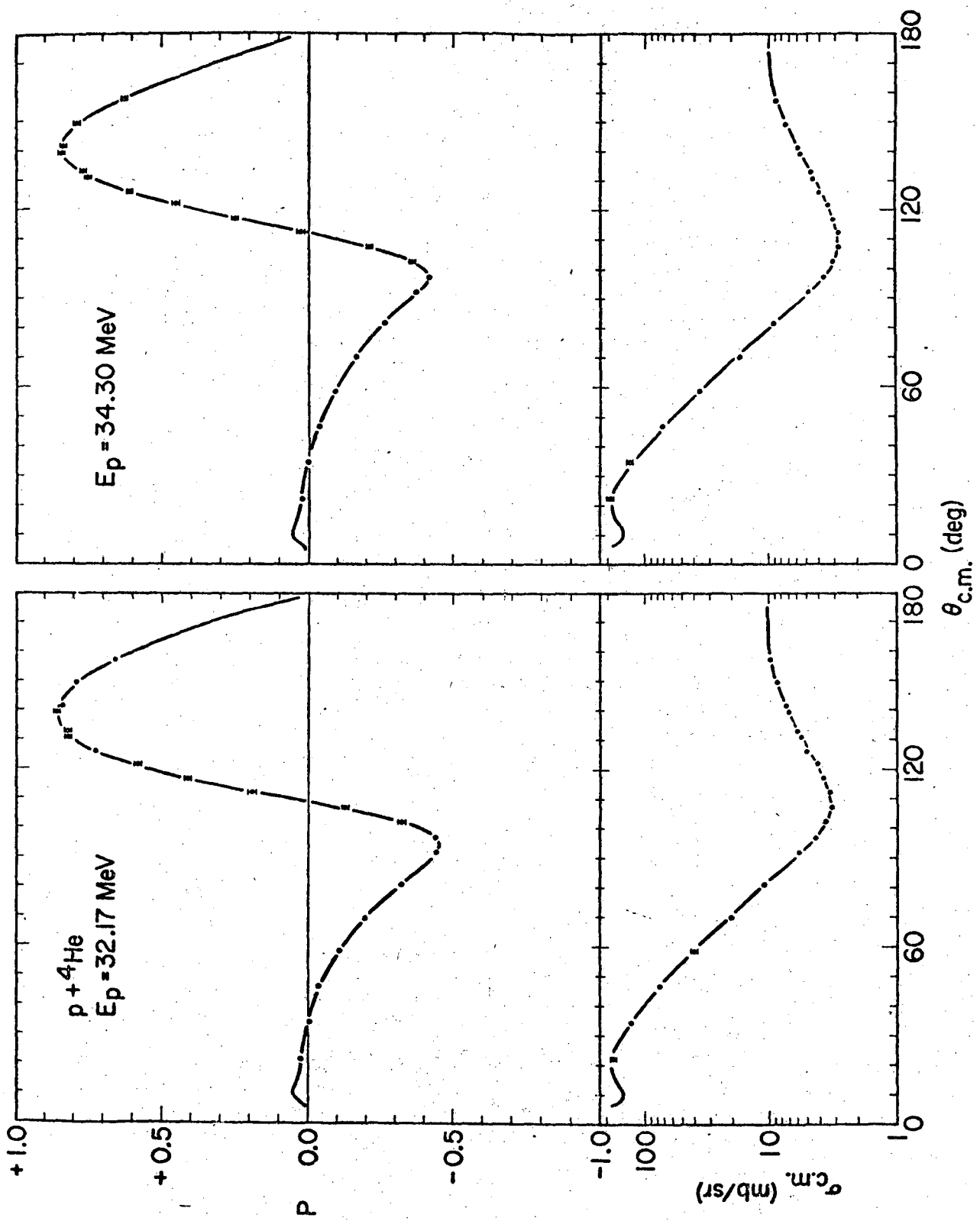
p + 4He
Ep = 32.17 MeV
Ep = 34.30 MeV
P
σc.m. (mb/sr)
θc.m. (deg)
+1.0
+0.5
0.0
-0.5
-1.0
100
10
1
0
60
120
180

Fig. 6

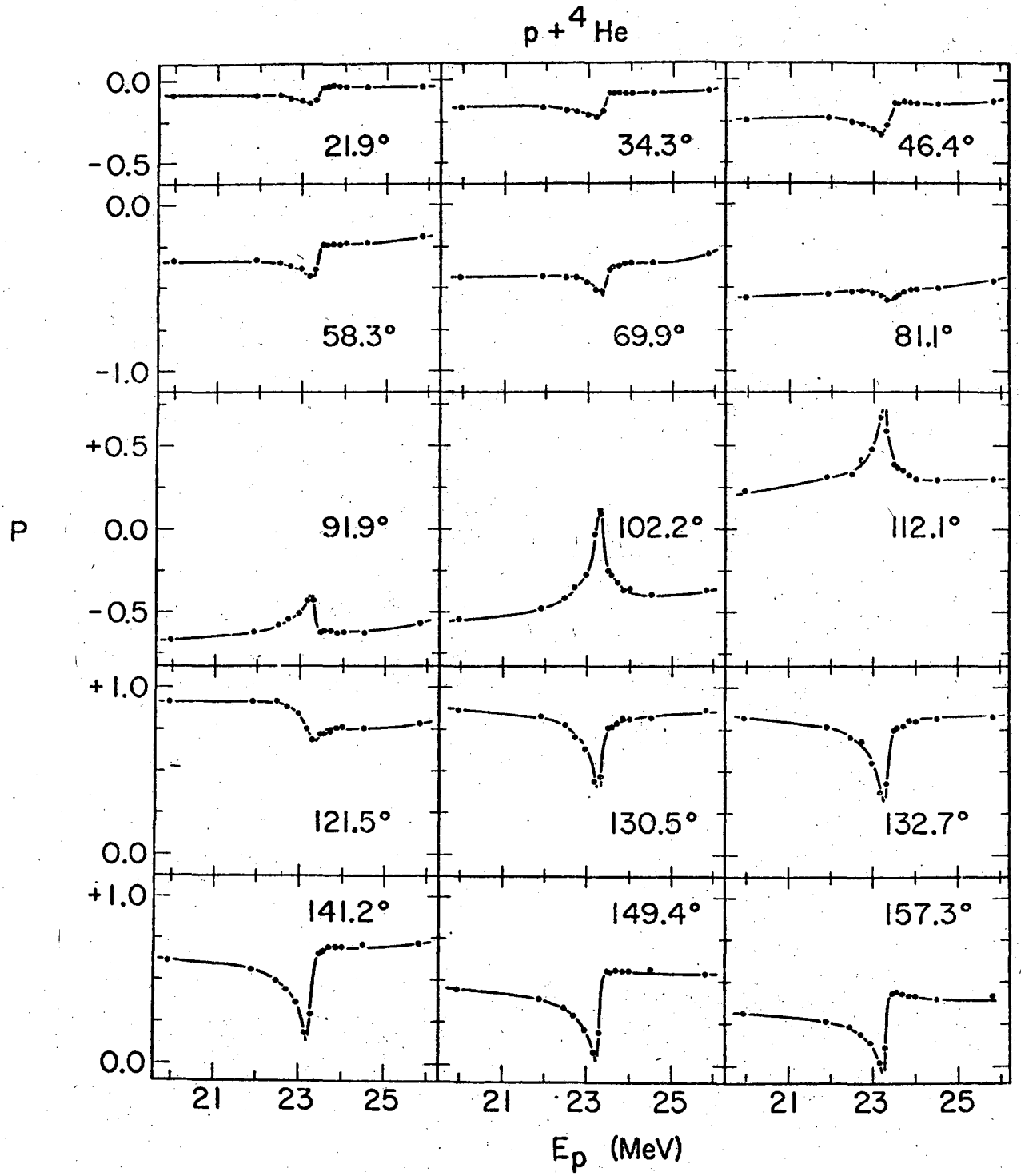
p + 4 He
21.9°
34.3°
46.4°
58.3°
69.9°
81.1°
91.9°
102.2°
112.1°
121.5°
130.5°
132.7°
141.2°
149.4°
157.3°
0.0
-0.5
-1.0
+0.5
+1.0
P
21
23
25
Ep (MeV)

Fig. 7

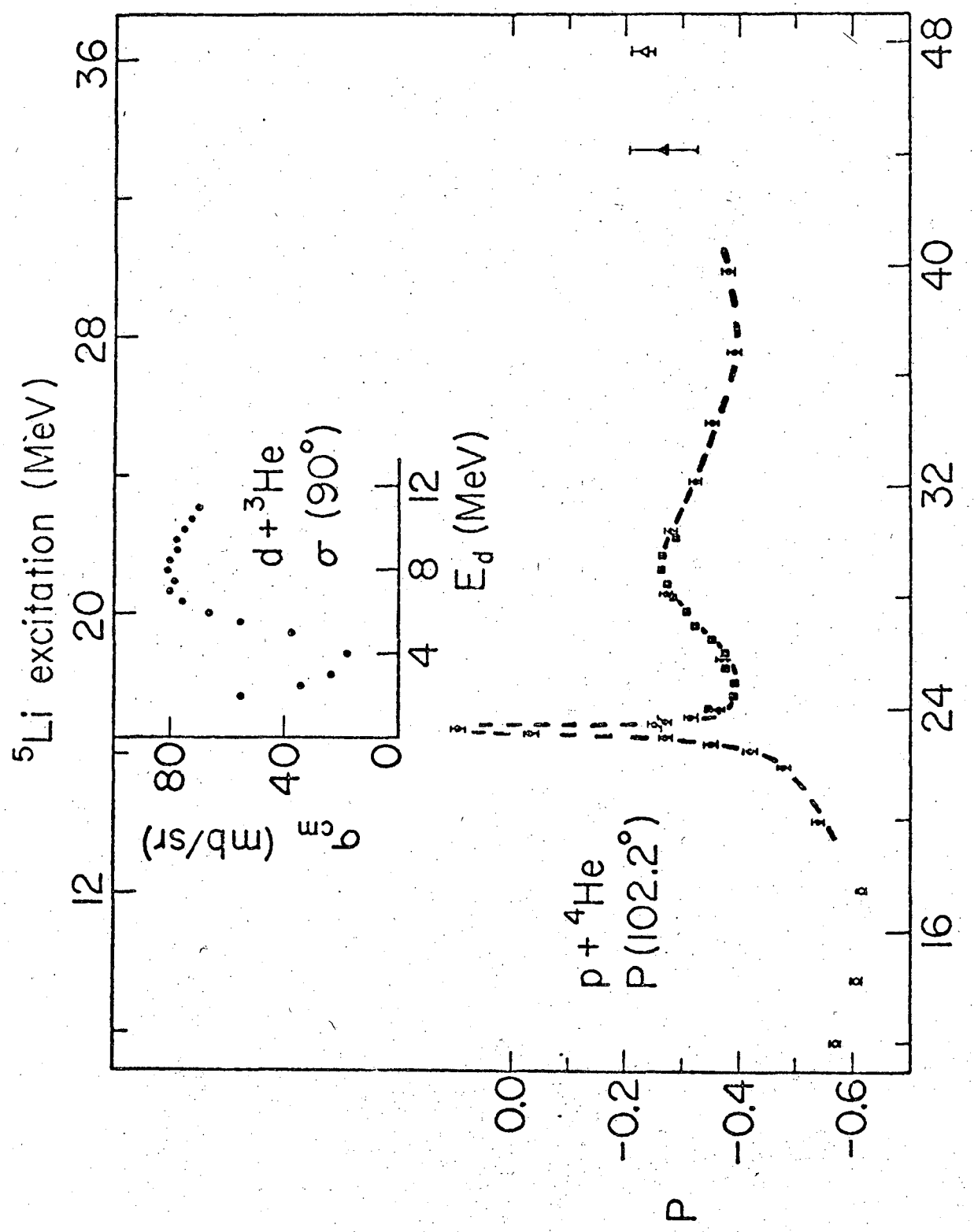
^{5}Li excitation (MeV)
12
20
28
36
E_p (MeV)
16
24
32
40
48
P
0.0
-0.2
-0.4
-0.6
p + ^{4}He
P (102.2°)
E_d (MeV)
4
8
12
σ_{cm} (mb/sr)
0
40
80
d + ^{3}He
σ (90°)

Fig. 8

TECHNICAL INFORMATION DIVISION
LAWRENCE BERKELEY LABORATORY
UNIVERSITY OF CALIFORNIA
BERKELEY, CALIFORNIA 94720